UMYU Scientifica, Vol. 3 NO. 4, December 2024, Pp 218 – 231
https://doi.org/10.56919/usci.2434.017
ISSN: 2955 – 1145 (print); 2955 – 1153 (online)
A periodical of the Faculty of Natural and Applied Sciences, UMYU, Katsina

ORIGINAL RESEARCH ARTICLE

Effect of Variable Thermal Conductivity on Oscillatory Magnetized Couette Flow in a Channel Filled with Porous Material

M. M. Hamza[1], O. J. Ejiwole[2], H. Usman[3], A. Almu[4], Aminu Hamisu[5] and Muawiya Musa[6]

[1]Department of Mathematics, Usmanu Danfodiyo University, Sokoto, Nigeria
[2]Department of Mathematics and Statistics, Federal Polytechnic Kaura Namoda, Zamfara State, Nigeria
[3]Department of Mathematics, Usmanu Danfodiyo University, Sokoto, Nigeria
[4]Department of Computer, Usmanu Danfodiyo University, Sokoto, Nigeria
[5]Department of Mathematics and Statistics, Umaru Musa Yar'adua University, Katsina, Nigeria
[6]Department of Motor Vehicles Mechanic, Idris Koko Technical School Farfaru, Sokoto, Nigeria

ARTICLE HISTORY

Received August 17, 2024
Accepted October 20, 2024
Published October 30, 2024

KEYWORDS

Oscillatory Flow, Magnetized Flow, Couette Flow, Porous Material, Variable Thermal Conductivity

© The authors. This is an Open Access article distributed under the terms of the Creative Commons Attribution 4.0 License (https://creativecommons.org/licenses/by-nc/4.0/)

ABSTRACT

The primary purpose of this study is to determine how temperature-dependent thermal properties affect oscillatory magnetic Couette fluid flows in a channel containing porous materials. A regular perturbation approach was used to analytically characterize the flow fluid boundary conditions of the governing equations. The expressions of velocity, temperature, concentration, skin friction, Nusselt number, and Sherwood number have been obtained, and the results are displayed graphically for various controlling parameters of the models. The results show that varying thermal conductivity on fluid flow of the model of both Nu_0 and Nu_1 enhanced heat transfer efficiency, reduction in thermal boundary layer thickness of the fluid leading to an increase in convective heat transfer coefficient and increase in the temperature gradients near the bottom plate and near the top plate respectively.

INTRODUCTION

Throughout history, humans have been attracted to areas with accessible fluid dynamics to establish communities and civilizations. As our knowledge of the natural world has advanced, we have endeavored to manage and enhance natural fluid flow to improve agricultural stability, living conditions, and transportation systems. By harnessing the power of fluid dynamics, we now live in a higher quality of life, sustain communities, and create more efficiency in the communities (Karwa 2020).

The manner in which electrically conducting liquids like plasma and liquid metallic substances behave while exposed to magnetic fields is known as magnetohydrodynamics (MHD). In nature, MHD describes the changes and behaviors of fluids when exposed to magnetic fields. There are several industries where MHD is applicable, including advanced propulsion systems and nuclear fusion energy production (Romanelli *et al.* 2017). MHD fluids have proven to be quite beneficial in the area of hemodynamics (the study of the human body to identify drug delivery techniques), biomedical sciences, vascular blood flow, cancer treatment (chemotherapy), and blood artery flow regulation (Falade *et al.* 2017).

Several mathematicians have studied MHD oscillatory fluids under the influence of magnetic fluid. The MHD fluid's effect on unstable oscillatory Couette flow in porous materials was described (Sharma *et al.*, 2022). Mass transfer and conversion heat are free to move across a semi-infinite vertical porous plate in unstable MHD fluids (Quader & Alam 2021). (Amos *et al.,* 2020) investigated the impact of varying viscosity and thermal conductivity in a Casson fluids heat transfer and chemically reacting MHD-free convective mass. (Rajashekar & Shankar 2016), Illustration of how chemical processes affect the unsteady MHD fluid flow of heat transfer and mass in semi-infinite vertical moving plates when they are exposed under the influence of a uniform magnet field with viscous and gradient temperatures. (Narsu & Rushikumar 2020) examined variable thermal conductivity and partial slips with radiated plates with unsteady magnetohydrodynamics chemically reactive fluid flows. The effects of heat on nanofluid at the stationary point and chemical changes on MHD fluid flow were determined (Anuradha & Priadhashini 2016) and (Gireesha & Rudraswamy 2014). The effects of changing thermal conductivity for power law separation related to concentration and temperature, as well as magnetic fields on mass and heat transfer, were discussed (Kareem & Salawu 2017). (Abiodun & Kabir

Correspondence: Ejiwole Oluwafemi Job. Department of Mathematics and Statistics, Federal Polytechnic Kaura Namoda, Zamfara State, Nigeria. ✉ enitioluwafe2012@gmail.com

How to cite: Hamza, M. M., Ejiwole, O. J., Usman, H., Almu, A., Hamisu, A., & Musa, M. (2024). Effect of Variable Thermal Conductivity on Oscillatory Magnetized Couette Flow in a Channel Filled with Porous Material. *UMYU Scientifica*, 3(4), 218 – 231. https://doi.org/10.56919/usci.2434.017

2020) explained the influence of thermal conductivity and variation over thermodynamic flow in vertical channels. (Uwanta and Usman 2015), Examined the finite difference method for MHD unrestricted convective flow of fluid over Drcy Forchheimer medium by suction and thermally variable conductivity. (Seddek *et. al.* 2007) Focused on the effect of suction and magnetic fields on unsteady MHD mass and heat transfer in a semi-infinite medium. (Babu *et al.* 2014) investigated the effects of radiation heat sources and sinks on stable two-dimensional layers through the mass suction and shrinking plate. The influences of suction and injection on the turbulent fluid in reactive viscous fluid through upward channels under the transfer of mass and heat were described by (Uwanta & Hamza 2014). (Zubi 2018) evaluated MHD mass and heat transfer on oscillation Couette flow through a chemical reaction in a porous material on an upward plate. Furthermore, (Prakash & Makinde 2015b) described how radiative heat transfer and a transversal magnetic field interact to cause an unstable flow. In a rotating system incorporating Hall effects, (Makinde *et al.* 2015) examined the thermodynamic implications of hydromagnetic flow in a varying viscosity. Moreover, (Prakash & Makinde 2015a) discusses how the velocity fluid, whether clean or dirty, is slowed down by the external magnetic field serving as a force that resists. Later on, his invention was thought to be helpful in sewage treatment plants, other real-life situations, and other industries. (Makinde *et al.* 2016) Examined the impacts of the chemical reaction using MHD poiseuille flow with nanofluids and the thermal radiative MHD oscillatory Couette flow in a vertical channel filled with permeable materials. (Agaie *et al.* 2020) determined the vertical porous channel with a plate oscillating in its plain and the other moving in the fluid flow direction. The impact of radiative hydromagnetic poiseuille fluid flow on two-step exothermic chemical reaction with convective cooling was examined by (Salawu *et al.* 2020).

Consequently, because of the industrial and practical application of heat energy in several fields like the dyeing industry, cooling technique gas and liquid industry, water evaporation, and separation of toxic and hazardous substances. The application of oscillatory Couette is very important in several fields of study in this modern era and it is significant in many different types of industries, such as petroleum, geothermal energy generation, and the advancement of advanced heat exchange techniques. The effect of heat energy transfer increases when oscillatory fluid flow is flowing, and it decreases when a fluid is kept stationary, and this is applicable in the fields of engineering and biomedicine variations in fluid velocity and patterns (Uddin and Murad, 2022).

When two parallel plates enclose a fluid, one is moving, and the other is held stationary in a fixed point by Stokes's first principle and it is called oscillatory Couette flow. This principle describes the use of fluid flows over a vertical channel at rest and quickly accelerates in its plane with constant velocity by Khaled & Vafai (2004) and Zulkarmain & Sharudin (2022). The motion of incompressible semi-finite viscous fluids caused by an oscillating plate is known as Skoke's second problem Umavathi & Beg (2020). A particular kind of fluid flow between two parallel plates that oscillates on a regular basis is called oscillatory Couette flow, and this process involves the periodic upward and downward movement of a fluid layer trapped between two plates (Noor *et al.* 2021, 2022)

The problem of oscillatory Couette fluid flow into a channel filled with permeable materials in different variable conditions has been tackled by numerous authors. This contemporary research seeks to fill the gap with the precedent literature work. We examined the study of the effect of variable thermal conductivity on oscillatory magnetized couette flow in a channel filled with a porous material. The set of second-order partial differential equations (PDEs) was solved analytically by regular perturbation method to convert the second-order partial differential equations to the ordinary differential equations due to the nature of the boundary condition oscillating. The study holds immense significance in both scientific exploration and in practical real-life applications, such as in oil recovery, rocket engines, designing of heat exchangers, to understand the interaction between fluid dynamics, heat transfer, and porous structures in the presence of variable thermal properties. It is also used in the field of Biomedical Engineering for biological tissue treatment, such as cryosurgery and hyperthermia.

MATHEMATICAL MODEL AND BASIC EQUATIONS

To examine the unstable, incompressible, oscillatory magnetized Couette flow in a channel full of permeable materials by variable thermal conductivity. Varying values of thermal conductivity of the fluid flow and movement of one of the plates induced the flow motion. The first plate is shown in Figure 1 to be at position $y^* = 0$, oscillating at frequency ω^* with velocity $u^* = U_0 (1+\varepsilon e^{i\omega t})$, While a magnetic field is provided along the y^* axis, the second plate, at a distance $y^* = h$, is moving vertically along the x^* axis towards the direction of flow with a fixed velocity (Up*). The governing equations in dimensional form are as follows, in accordance with (Sharma *et al.* 2023):

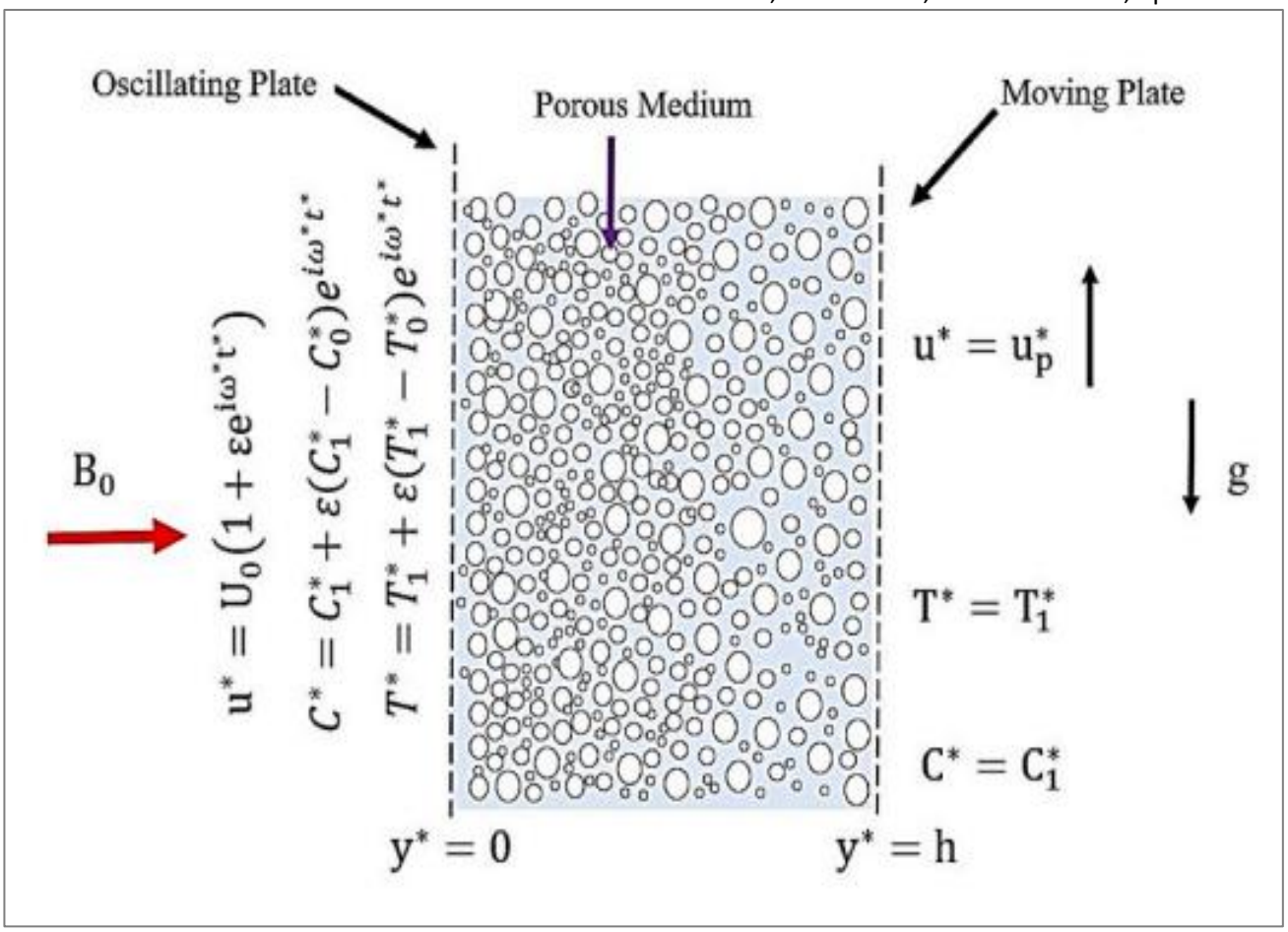

Figure 1: The flow Model

The continuity equation

$$\frac{\partial u^*}{\partial x^*} = 0 \tag{1}$$

Conservation of momentum or motion

$$\frac{\partial u^*}{\partial t^*} = v\frac{\partial^2 u^*}{\partial y^{*2}} - \frac{v}{K^*}u^* + g\beta(T^* - T_0^*) + g\beta^*(C^* - C_0^*) - \frac{\sigma\beta_0^2}{\rho}u^* \tag{2}$$

Heat conservation

$$\frac{\partial T^*}{\partial t^*} = \frac{1}{\rho Cp}\frac{\partial}{\partial y^*}\left(K_f\frac{\partial T^*}{\partial y^*}\right) - \frac{1}{\rho Cp}\left(\frac{\partial q_r^*}{\partial y^*}\right) \tag{3}$$

Conservation of concentration

$$\frac{\partial C^*}{\partial t^*} = Dm\frac{\partial^2 C^*}{\partial y^{*2}} + K_R(C^* - C_0^*) \tag{4}$$

The boundary constraints are:

$U^* = U_0(1 + e^{i\omega^* t^*})$, $C^* = C_1^* + \varepsilon(C_1^* - C_0^*)e^{i\omega^* t^*}$, $T^* = T_1^* + \varepsilon(T_1^* - T_0^*)e^{i\omega^* t^*}$; $y^* = 0$;

$U^* = u_q^*$, $C^* = C_1^*$, $T^* = T_1^*$ $y^* = h$; (5)

Sharma *et al.* (2023). The below model represents the heat flux

$$\frac{\partial q_r^*}{\partial y^*} = 4(T^* - T_0^*)\int_0^\infty K_{\lambda w}\left(\frac{\partial e_{b\lambda}}{\partial T}\right)_w d\lambda = 4\alpha^2(T^* - T_1^*). \quad 6$$

The following are the non-dimensional parameters and the physical quantities.

$$y=\frac{y*}{h}, \omega=\frac{h^2\omega^*}{v},\ T=\frac{T^*-T_1^*}{T_1^*-T_0^*},\ u_q=\frac{u_q^*}{U_0},\ u=\frac{u*}{U_0},\ t=\frac{t^*v}{h^2}, M=\frac{\sigma B_0^* h^2}{\rho v},\ R=\frac{4\alpha^2 h^2}{k}, v=\frac{\mu}{\rho},$$

$$K_R=\frac{k_c h^2}{v}, \quad Pr=\frac{\mu Cp}{\kappa}, K=\frac{h^2}{K^*} Gr=\frac{g\beta h^2(T_1^*-T_0^*)}{vU_0}, \quad Gc=\frac{g\beta h^2(C_1^*-C_0^*)}{vU_0},$$

$$C=\frac{C^*-C_0^*}{C_1^*-C_0^*},\ Sc=\frac{v}{D_m}, \quad 7$$

Basic Assumptions

The following assumptions are considered under the preset research work:

i. The fluid is viscous, incompressible and electrically conducting oscillatory Couette flow.

ii. The temperature of the fluid and solid phase are equal in a channel filled with porous materials.

iii. There is uniform magnetic field, and thermal radiation saturated with porous medium bounded between two infinite thin plates.

iv. The flow is laminar and fully developed.

v. It is assumed that the fluid has both constant and variable thermal conductivity and viscosity.

Method of Solution

The solution was obtained by first substituting the equation. (6) into (3), then equation. (7) is substituted into (2)–(4) to have the dimensionless form equation (8) – (10).

$$\frac{\partial U}{\partial t} = \frac{\partial^2 U}{\partial y^2} - (K+M)U + GrT + GcC \quad 8$$

$$\Pr\frac{\partial T}{\partial t} = (1+VmT)\frac{\partial^2 T}{\partial y^2} + Vm\left(\frac{\partial u}{\partial y}\right)^2 - RT \quad 9$$

$$Sc\frac{\partial C}{\partial t} = \frac{\partial^2 C}{\partial y^2} + K_R S_c C \quad 10$$

The dimensionless boundary conditions were reduced to equation (11)

$$\left.\begin{aligned} U &= 1+\varepsilon e^{iwt},\ T = 1+\varepsilon e^{iwt},\ = 1+\varepsilon e^{iwt}, \quad y = 0 \\ U &= u_{p,}\quad T = 1\ ,\ C = 1 \end{aligned}\right\} \quad 11$$

The equation $\eta(y,t) = \eta_0(y) + \varepsilon e^{i\omega t}\eta_1(y) + O(\varepsilon^2)$ for small amplitudes is used to reduce the PDEs into ODEs because the equations are second-order PDEs with two independent variables y and t, which at this stage, the solution of these equations are not possible to solve. Where η is a symbolic representation of concentration C, temperature T, velocity U, and the higher order of ε is neglected.

$$\left.\begin{aligned} U &= U_0 + \varepsilon U_1 e^{iwt} \\ T &= T_0 + \varepsilon T_1 e^{iwt} \\ C &= C_0 + \varepsilon C_1 e^{iwt} \end{aligned}\right\} \quad 12$$

Equation (13) is the concentrated equation from equation (12)

$$C = A_1 \cos\left(\sqrt{\alpha_1}\, y\right) + A_2 \sin\left(\sqrt{\alpha_1}\, y\right) + \varepsilon\left[A_3 \cos\left(\sqrt{\alpha_2}\, y\right) + A_4 \sin\left(\sqrt{\alpha_2}\, y\right)\right] e^{iwt} \quad 13$$

To obtain the temperature equation, the regular perturbation on perturbation was used from equation (9) to have equations (14) and (15)

$$T_0'' + VmT_0\, T_0'' + Vm\left(T_0'\right)^2 - RT_0 = 0 \quad 14$$

$$T_1'' + VmT_0\, T_1'' + 2VmT_0'' T_1' - \left(P_r iw + R\right)T_1 = 0 \quad 15$$

Boundary conditions for equation (14) and (15)

$$\left.\begin{aligned} &T_0 = 1;\ T_1 = 1 \quad at \quad y = 0 \\ &T_0 = 1;\ T_1 = 0 \quad at \quad y = 1 \\ &let \\ &T_0 = T_{00} + VmT_{01} \\ &T_1 = T_{11} + VmT_{12} \end{aligned}\right\} \quad 17$$

Equation (17) was then substituted into equations. (14), (15) to have equation (18)

$$\left.\begin{aligned} &T_{00}' - RT_{00} = 0 \\ &T_{00}'' - RT_{01} = -T_{00}\, T_{00}'' - \left[T_{00}'\right]^2 \\ &T_{11}'' - \alpha_3 T_{11} = 0 \\ &T_{12}'' - \alpha_3 T_{12} = -T_{00}\, T_{11}'' - 2T_{00}'\, T_{11}' \end{aligned}\right\} \quad 18$$

The following boundary conditions are used

$$\left.\begin{aligned} &T_{00} = 1;\ T_{01} = 0;\ T_{11} = 1; T_{12} = 0;\ \ at\ y = 0 \\ &T_{00} = 1;\ T_{01} = 0;\ T_{11} = 0;\ T_{12} = 0;\ \ at\ y = 0 \end{aligned}\right\} \quad 19$$

The solutions for equation (18) were subjected to equation (19) to obtain equation (20) – (23):

$$T_{00} = B_1 e^{y\sqrt{R}} + B_2 e^{-y\sqrt{R}} \quad 20$$

$$T_{01} = \left(B_3 + B_5\right) e^{2y\sqrt{R}} + \left(B_4 + B_6\right) e^{-2y\sqrt{R}} \quad 21$$

$$T_{11} = B_7 e^{y\sqrt{\alpha_3}} + B_8 e^{-y\sqrt{\alpha_3}} \quad 22$$

$$T_{12} = B_9 e^{y\sqrt{\alpha_3}} + B_{10} e^{-y\sqrt{\alpha_3}} + B_{11} e^{y\alpha_4} + B_{12} e^{-y\alpha_4} + B_{13} e^{y\alpha_5} + B_{14} e^{y\alpha_6} \quad 23$$

Equation (20) – (23) were substituted into equation (18) with equation (12) to have equation (24) the Temperature (T) equation

$$T = B_1 e^{y\sqrt{R}} + B_2 e^{-y\sqrt{R}} + V_m\left[\left(B_3 + B_5\right)e^{2y\sqrt{R}} + \left(B_4 + B_6\right)e^{-2y\sqrt{R}}\right] +$$
$$\varepsilon\left[\left(B_7 e^{y\sqrt{\alpha_3}} + B_8 e^{-y\sqrt{\alpha_3}}\right) + V_m\left(B_9 e^{y\sqrt{\alpha_3}} + B_{10} e^{-y\sqrt{\alpha_3}} + B_{11} e^{y\alpha_4} + B_{12} e^{-y\alpha_4} + B_{13} e^{y\alpha_5} + B_{14} e^{y\alpha_6}\right)\right] e^{iwt} \quad 24$$

Solving equation (8) to obtain equations (25) and (26)

$$U_0 = D_1 e^{y\sqrt{H_1}} + D_2 e^{-y\sqrt{H_1}} + D_3 e^{y\sqrt{R}} + D_4 e^{-y\sqrt{R}} + D_5 \cos\left(\sqrt{\alpha_1}\, y\right) + D_6 \sin\left(\sqrt{\alpha_1}\, y\right) + D_6^* e^{2y\sqrt{R}} + D_7^* e^{-2y\sqrt{R}} \quad 25$$

$$U_1 = D_7 e^{y\sqrt{H_2}} + D_8 e^{-y\sqrt{H_2}} + D_9 e^{y\sqrt{\alpha_3}} + D_{10} e^{-y\sqrt{\alpha_3}} + D_{11} e^{y\alpha_4} + D_{12} e^{-y\alpha_4} + D_{13} e^{y\alpha_5} + D_{14} e^{y\alpha_6} + D_{15} \cos\left(\sqrt{\alpha_2}\, y\right) + D_{16} \sin\left(\sqrt{\alpha_2}\, y\right) \quad 26$$

Equation (25) and (26) was substituted into equation (12) to have equation (27) the Velocity equation (U)

$$U = D_1 e^{y\sqrt{H_1}} + D_2 e^{-y\sqrt{H_1}} + D_3 e^{y\sqrt{R}} + D_4 e^{-y\sqrt{R}} + D_5 \cos\left(\sqrt{\alpha_1}\, y\right) + D_6 \sin\left(\sqrt{\alpha_1}\, y\right) + D_6^* e^{2y\sqrt{R}} + D_7^* e^{-2y\sqrt{R}} +$$
$$\varepsilon\left(D_7 e^{y\sqrt{H_2}} + D_8 e^{-y\sqrt{H_2}} + D_9 e^{y\sqrt{\alpha_3}} + D_{10} e^{-y\sqrt{\alpha_3}} + D_{11} e^{y\alpha_4} + D_{12} e^{-y\alpha_4} + D_{13} e^{y\alpha_5} + D_{14} e^{y\alpha_6} + D_{15} \cos\left(\sqrt{\alpha_2}\, y\right) + D_{16} \sin\left(\sqrt{\alpha_2}\, y\right)\right) e^{iwt} \quad 27$$

In equations (28) and (29), the Nusselt number was obtained by differentiating equation (24) with respect to y at y = 0 and 1, respectively,

$$\left.\frac{dT}{dy}\right|_{y=0} = B_1\sqrt{R} - B_2\sqrt{R} + 2VmB_3^*\sqrt{R} - 2VmB_4^*\sqrt{R} + \varepsilon\begin{bmatrix} B_7\sqrt{\alpha_3} - B_8\sqrt{\alpha_3} + 2VmB_9\sqrt{\alpha_3} - VmB_{10}\sqrt{\alpha_3} + \\ VmB_{11}\alpha_4 - VmB_{12}\alpha_4 + VmB_{13}\alpha_5 + VmB_{14}\alpha_6 \end{bmatrix} e^{iwt} \quad 28$$

$$\left.\frac{dT}{dy}\right|_{y=1} = B_1\sqrt{R}e^{\sqrt{R}} - B_2\sqrt{R}e^{-\sqrt{R}} + 2VmB_3^*\sqrt{R}e^{2\sqrt{R}} - 2VmB_4^*\sqrt{R}e^{-2\sqrt{R}} + \varepsilon\begin{bmatrix} B_7\sqrt{\alpha_3}e^{\sqrt{\alpha_3}} - B_8\sqrt{\alpha_3}e^{-\sqrt{\alpha_3}} + VmB_9\sqrt{\alpha_3}e^{\sqrt{\alpha_3}} - VmB_{10}\sqrt{\alpha_3}e^{-\sqrt{\alpha_3}} \\ + VmB_{11}\alpha_4 e^{\alpha_4} - VmB_{12}\alpha_4 e^{-\alpha_4} + VmB_{13}\alpha_5 e^{\alpha_5} + VmB_{14}\alpha_6 e^{\alpha_6} \end{bmatrix} e^{iwt} \quad 29$$

In equations (30) and (31), the Skin Friction was obtained by differentiating equation (27) with respect to y at y = 0 and 1, respectively

$$\left.\frac{dU}{dy}\right|_{y=0} = D_1\sqrt{H_1} - D_2\sqrt{H_1} + D_3\sqrt{R} - D_4\sqrt{R} + 2\sqrt{R}D_6^* - 2\sqrt{R}D_7^* + D_6\sqrt{\alpha_1} + \varepsilon\begin{bmatrix} D_7\sqrt{H_2} - D_8\sqrt{H_2} + D_9\sqrt{\alpha_3} - D_{10}\sqrt{\alpha_3} \\ + D_{11}\alpha_4 - D_{12}\alpha_4 + D_{13}\alpha_5 + D_{14}\alpha_6 + D_{16}\sqrt{\alpha_2} \end{bmatrix} e^{iwt} \quad 30$$

$$\left.\frac{dU}{dy}\right|_{y=1} = D_1\sqrt{H_1}e^{\sqrt{H_1}} - D_2\sqrt{H_1}e^{-\sqrt{H_1}} + D_3\sqrt{R}e^{\sqrt{R}} - D_4\sqrt{R}\,e^{-\sqrt{R}} - D_5\sqrt{\alpha_1}\sin\left(\sqrt{\alpha_1}\right) + D_6\sqrt{\alpha_1}\cos\left(\sqrt{\alpha_1}\right) + 2D_6^*\sqrt{R}\,e^{2\sqrt{R}} - 2D_7^*\sqrt{R}\,e^{-2\sqrt{R}} +$$

$$\varepsilon\begin{bmatrix} D_7\sqrt{H_2}\,e^{\sqrt{H_2}} - D_8\sqrt{H_2}\,e^{-\sqrt{H_2}} + D_9\sqrt{\alpha_3}\,e^{\sqrt{\alpha_3}} - D_{10}\sqrt{\alpha_3}e^{-\sqrt{\alpha_3}} \\ + D_{11}\alpha_4 e^{\alpha_4} - D_{12}\alpha_4 e^{-\alpha_4} + D_{13}\alpha_5\,e^{\alpha_5} + D_{14}\alpha_6 e^{\alpha_6} \\ -D_{15}\sqrt{\alpha_2}\sin(\sqrt{\alpha_2}) + D_{16}\sqrt{\alpha_2}\cos(\sqrt{\alpha_2}) \end{bmatrix} e^{iwt} \quad 31$$

In equations (32) and (33), the Sherwood number was obtained by differentiating equation (13) with respect to y at y = 0 and 1, respectively.

$$\left.\frac{dC}{dy}\right|_{y=0} = A_2\sqrt{\alpha_1} + \varepsilon\left[A_4\sqrt{\alpha_2}\right]e^{iwt} \quad 32$$

$$\left.\frac{dC}{dy}\right|_{y=1} = -A_1\sqrt{\alpha_1}\sin(\sqrt{\alpha_1}) + A_2\sqrt{\alpha_1}\cos(\sqrt{\alpha_1}) + \varepsilon\left[-A_3\sqrt{\alpha_2}\sin(\sqrt{\alpha_2}) + A_4\sqrt{\alpha_2}\cos(\sqrt{\alpha_2})\right]e^{iwt} \quad 33$$

RESULTS AND DISCUSSIONS

To determine how temperature-dependent heat conductivity affects oscillatory magnetized Couette flow in a porous material-filled vertical channel, a Regular perturbation approach was employed to solve the governing equations. The key parameters governing the flow include the Magnetic field (M), Thermal Grashof number (Gr), Schmidt number (Sc), and Prandtl number (Pr). The oscillation frequency (ω), The porous media's permeability (K), parameter for chemical reactions (KR), and the Heat Radiation parameter (R). Following Sharma *et al.* (2023), we used specific values for example, Pr = 0.03 (mercury), Pr = 0.71 (air), Pr = 7.0 (water), Sc = 0.22 (hydrogen), Sc = 0.60 (water), and Sc = 1.16 (acetic acid) for the Prandtl number (Pr) and Schmidt number (Sc) in this model. The moving plate velocity and perturbation parameters were set to 0.75 m/s and $\varepsilon = 0.25\ (<<1)$. respectively.

Transient Patterns of Temperature, Concentration and Velocity:

Figures 2(a) and 2(b) show the impact of permeability (K) and magnetic field (M) parameters on the velocity profile. The velocity fluid profile was discovered to decrease while permeability parameters (K = 0.1, 0.2, 0.3) improved due to higher permeability porous materials enabling easier fluid flow 2(a). Likewise, a drop in the fluid velocity profile was noticed by raising the parameter for the magnetic field (M = 1, 2, and 3), confirming that magnetic fields possessed a negative influence on fluid velocity. The buoyancy forces (Gr and Gc) with an impact on the fluid velocity profile are shown in Figures 3(a) and 3(b). A rise has been observed for various Local Grashof values for numbers (Gr and Gc) on the profile of fluid velocity. An increasing trend is observed for different ranges of the local Grashof number (Gr and Gc = 0.1, 0.5, and 1.0). The velocity fluid profile shows stronger buoyant forces, which advance with an increase in the local Grashof number. Figures 4(a) and 4(b) indicate how changing thermal conductivity (Vm) affects velocity and temperature profiles. Whereby increasing values of the profiles of temperature and velocity are noticed with increasing Vm because the fluid particles' kinetic energy has increased. The impact of radiation parameters (R) on temperature and velocity profiles is seen in Figures 5(a) and 5(b). Unlike fluid motion due to increased thermal radiation, fluid velocity profiles decrease as R values (R = 1.0, 2.0, and 3.0) increase in the opposite direction to what is expected from fluid motion because of the higher thermal radiation parameters. As the radiation parameter values increase, the temperature profile shows a distinct behavior that is characterized by both acceleration and deceleration, as shown in Figure 5(b). Depending on the enclosure-specific operating conditions, this occurrence differs from velocity profiles and becomes more noticeable at higher temperatures. Figures 6(a) and 6 (b) illustrate how the Prandtl number (Pr) affects velocity and temperature profiles. Figure 6(a) illustrates how a decrease in velocity profiles is revealed for the following fluids at 20 °C when the Prandtl number increases. With a maximal decrease in the middle of the fluid temperature profile in Pr = 0.03 of mercury, P_r = 0.71 of air, and P_r = 7.0 of water. Since Pr regulates fluids' thermal boundaries with relative thickening of momentum. Figures 7(a) and 7(b) illustrate the nature of Chemical Reaction (K_R) on velocity and concentration profiles. Figure 7(a) demonstrates that increase in the flow of fluids

acceleration velocity fluid with an increase in K_R parameters (2.0, 4.0, and 8.0), while Figure 7(b) reveals that the concentration profiles accelerate most in the middle part of the channel due to the rearrangement of molecules or ions in a substance which accelerate the values of K_R values. Figures 8(a) and 8(b) exhibit how buoyant force (Sc) affects concentration and velocity profiles. Whereby different fluid levels exhibit a maximum rise in the concentration profile. Acetic acid (CH3COOH) (Sc = 1.16), hydrogen (H) (Sc = 0.22), and water (H2O) (Sc = 0.60), compared to the fluid's velocity profile when the buoyancy force ratio increases.

The impact of varying thermal conductivity (Vm) on the Prandtl number (Pr) at two different plate positions (y = 0 and y = 1) is shown in Figures 9 and 10. The behavior of different fluids at two plates with varying Vm values (0.01, 0.05, and 0.10) is depicted in the graph. A distinct pattern appears: skin friction increases as Vm, resulting in a large increase in both skin friction (T_0 and T_1). Moreover, an appreciable improvement in both Nusselt numbers (Nu_0 and Nu_1) at the corresponding plate is noticeable and is shown in Figures 10(a) and 10(b). These results highlight the significant effects, improved heat transfer efficiency, and Potential reduction in thermal boundary layer thickness of the fluid. Varying thermal conductivity on fluid flow dynamics of both Nu_0 and Nu_1 enhanced heat transfer, increasing the temperature gradients near the bottom plate and the top plate, respectively, with increased convective heat transfer coefficient. Comparing this work with other works, it was observed that higher Nu values enhanced better heat transfer performance. Figure 11 depicts the validation between the review of (Sharma *et al.* 2023) and this recent work when Vm = 0. It was observed that there is an agreement in both boundary conditions on the velocity axis and y-axis as the graph converges at a point (1) on this present work and the review work of (Sharma *et al.* 2023) at Vm = 0.

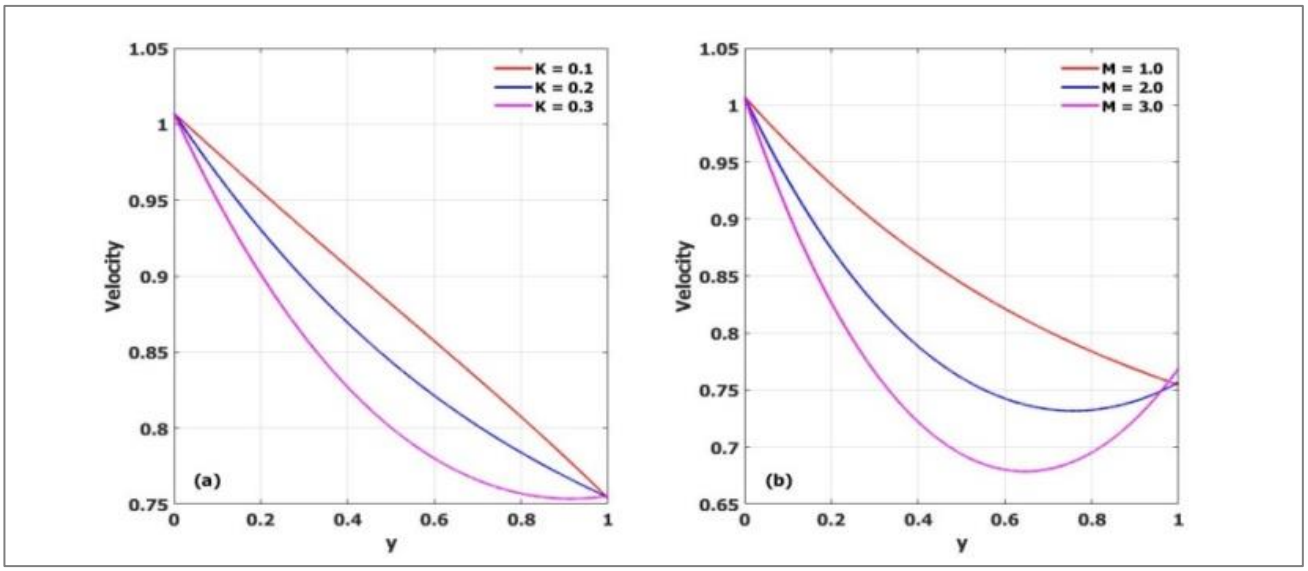

Figure 2: Effect of (a) permeability parameter (K) and (b) Magnetic field (M) on fluid velocity, u

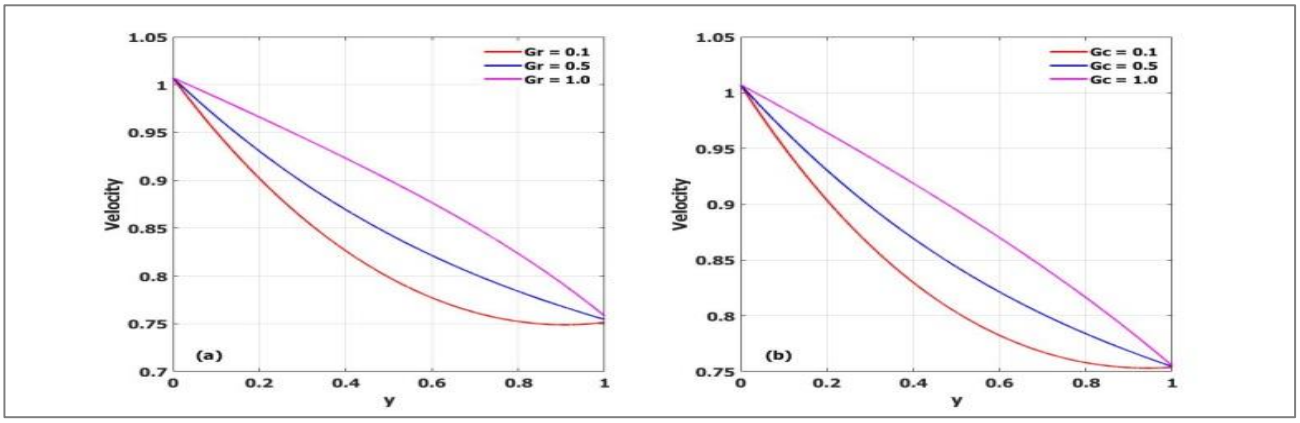

Figure 3: Shows how the Buoyancy forces: (a) (Gr) & (b) (Gc) affect the Velocity Profile

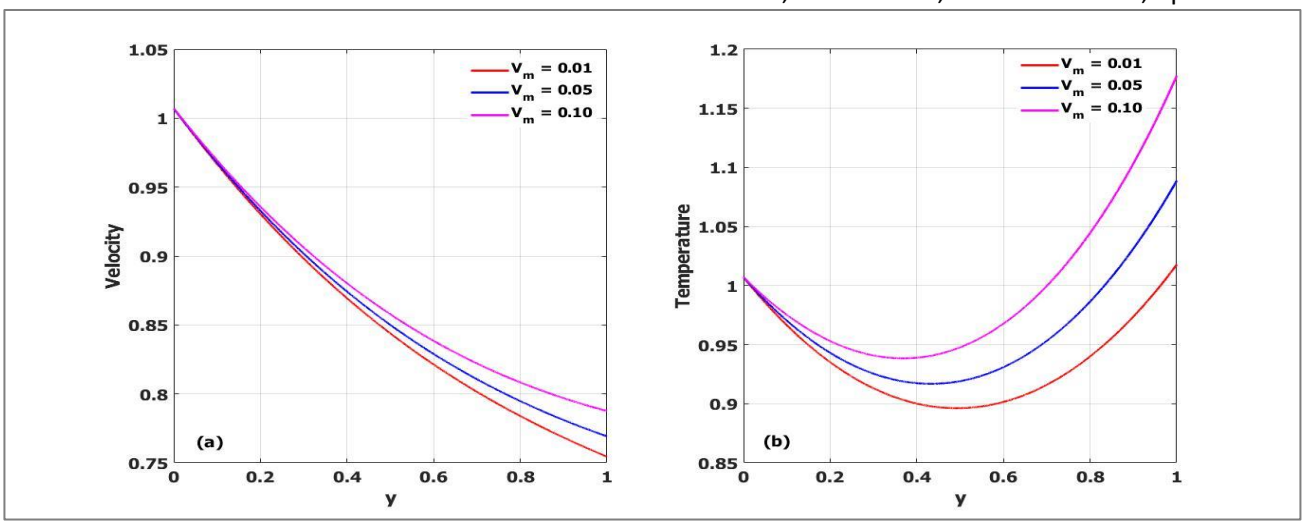

Figure 4: Impact of Variable Thermal Conductivity (Vm) on (a) Velocity and (b) Temperature Profiles.

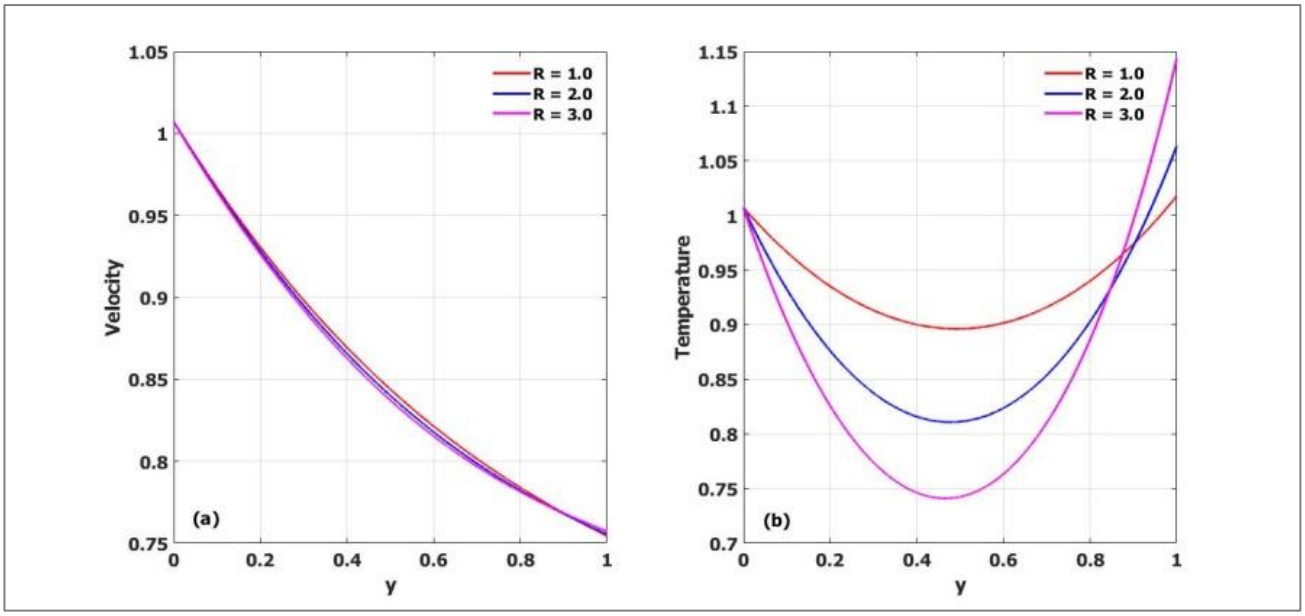

Figure 5: Effects of Radiation Parameter (R) on (a) Velocity and (b) Temperature Profiles.

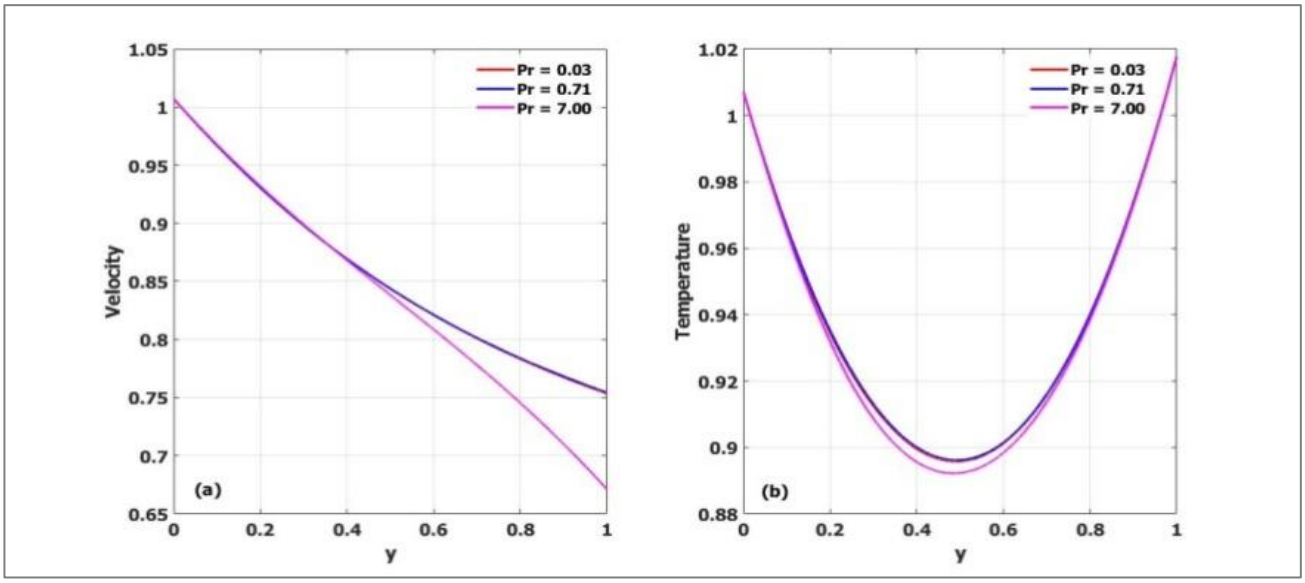

Figure 6: Impact of Prandtl number (Pr) on (a) Velocity and (b) Temperature Profiles.

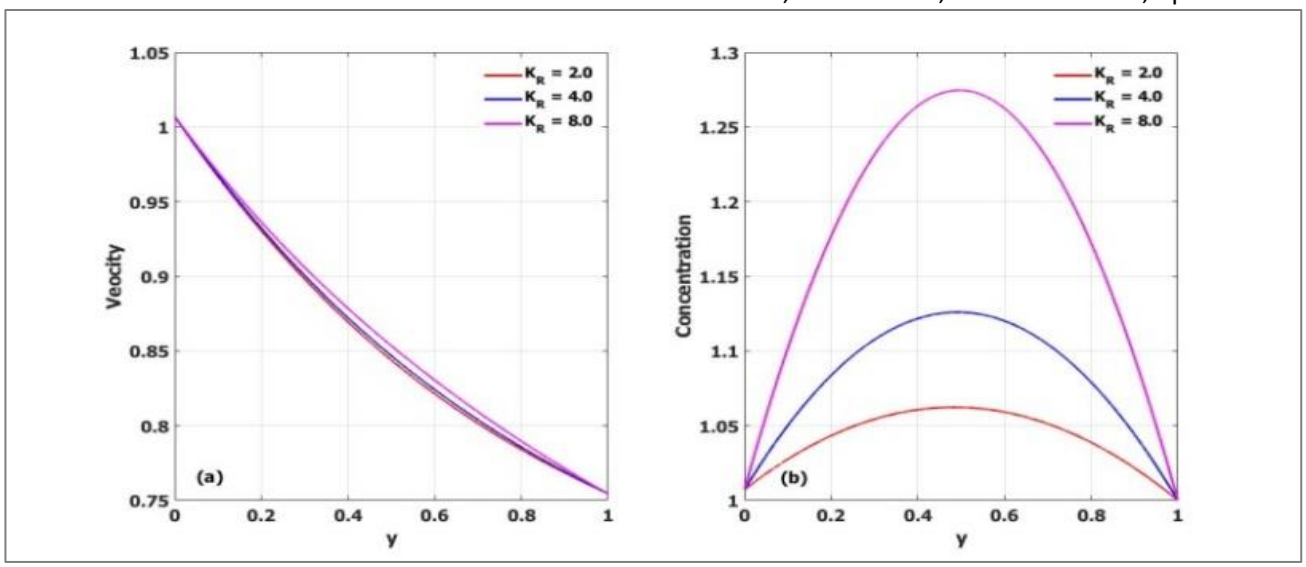

Figure 7: Shows the effects of Chemical reaction (K_R) on (a) Velocity and (b) Concentration Profile

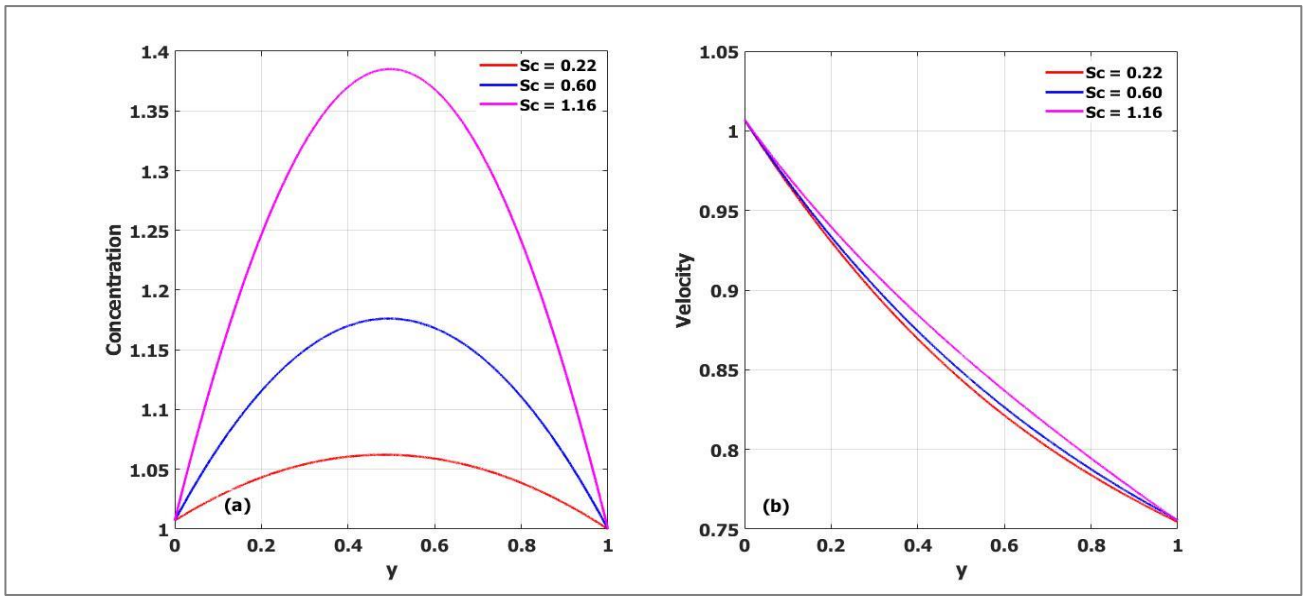

Figure 8: Effects of Buoyancy force (Sc) on (a) Concentration and (a) Velocity Profiles

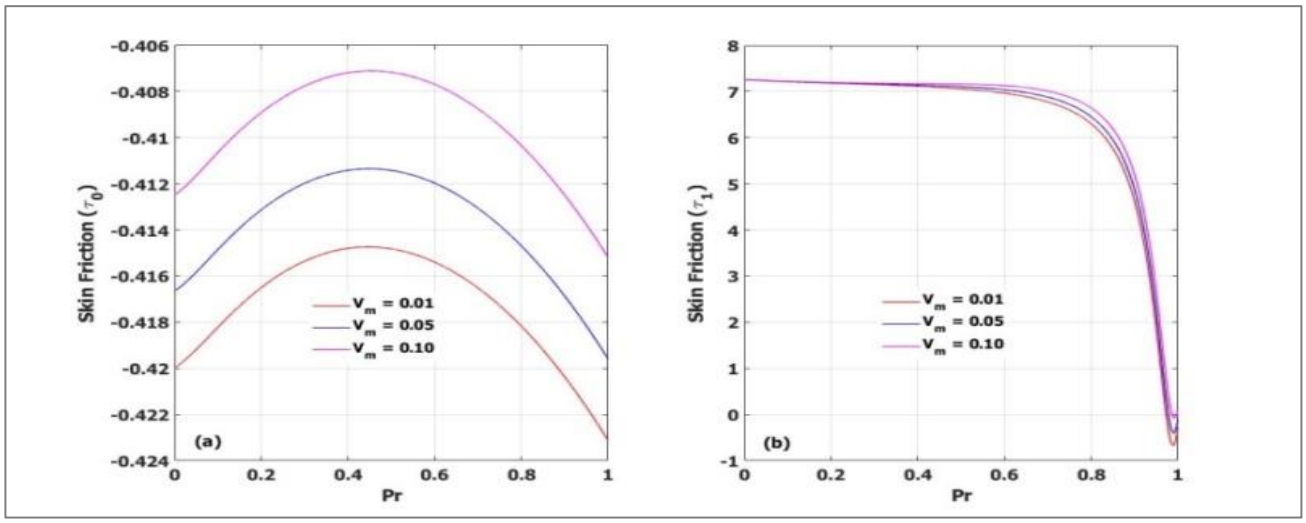

Figure 9: Effects variable thermal conductivity (V_m) against prandtl number (Pr) when y=1 and y = 0

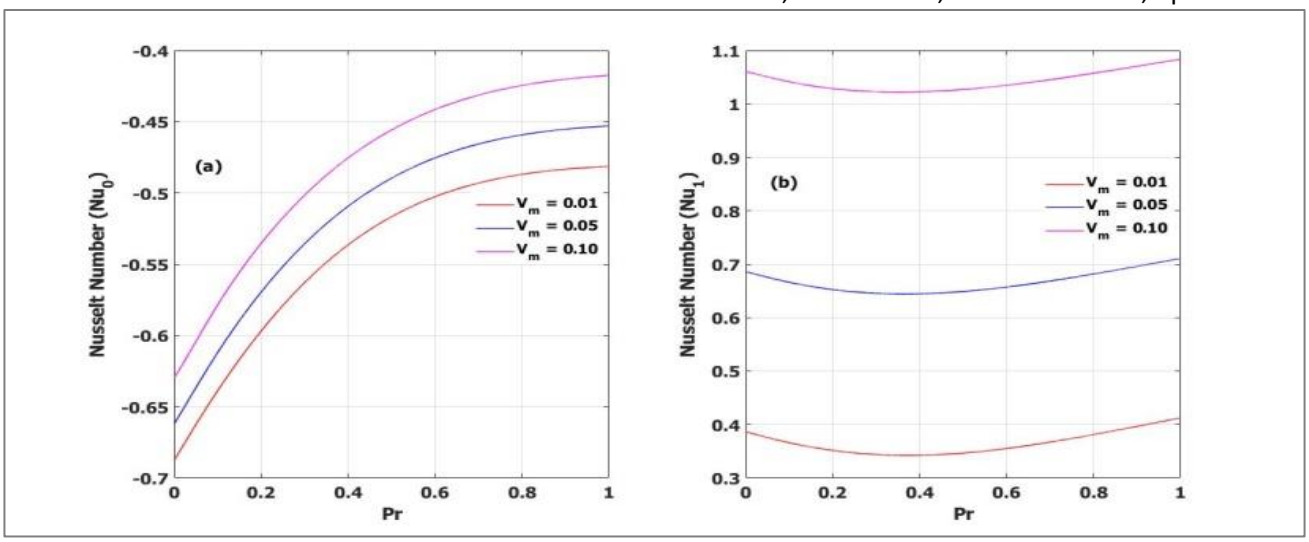

Figure 10: Effects of variable thermal conductivity (V_m) against prandtl number (Pr) when y = 1, y = 0

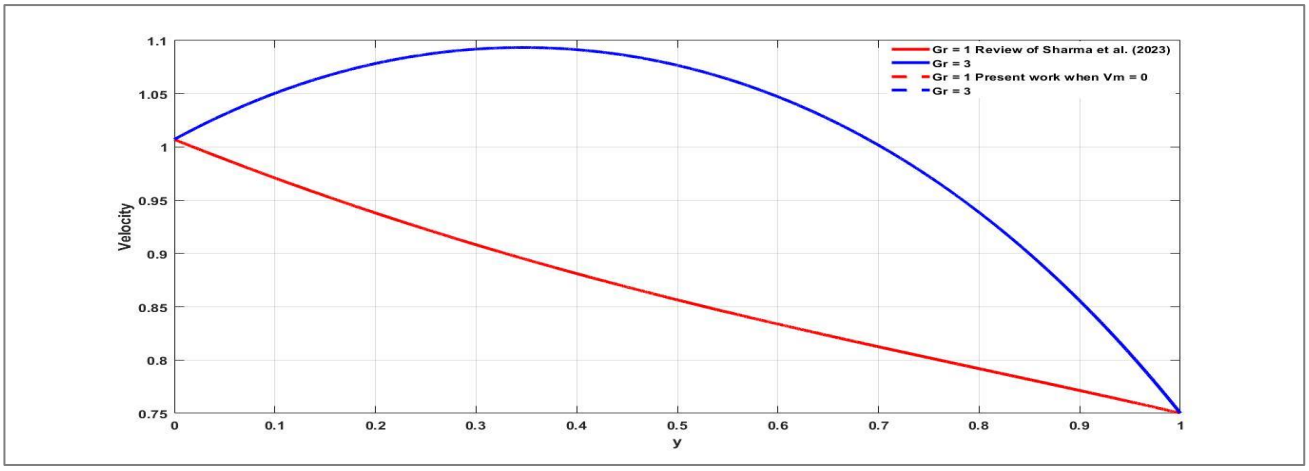

Figure 11: Comparison of review of Sharma *et al.* 2023 and the recent work when Vm = 0

CONCLUSIONS

This study investigated the effect of oscillatory magnetized Couette flow in a channel filled with porous material impacted by variable thermal conductivity. The regular perturbation approach was utilized and the transient governing equations are numerically solved. The visual illustrations of various fluid flow parameters, including temperature, velocity, concentration, skin friction, Sherwood number, and Nusselt number, were discussed. Key conclusions drawn from this study are outlined below:

i. The incorporation of variable thermal conductivity has a dual impact, enhancing fluid velocity while also modifying the temperature gradient within the fluid.

ii. The Nusselt number on the plates and skin friction rises with increasing variable thermal conductivity values.

iii. Compared to the Prandtl number of mercury, the Prandtl number of water causes a decline in fluid temperature and velocity.

iv. The Schmidt number of acetic acid results in reduction of both the concentration and velocity of the fluid than the relative Schmidt number of hydrogen. This finding has several practical applications, such as in chemical processing to design chemical reactors, pharmaceutical industry for drug delivery and coating, and in environmental engineering for accurate modeling of pollutant transport in water or air requires consideration of Schmidt number effects, food processing to improve texture, stability, and flavor and so on.

RECOMMENDATIONS

Based on these findings, the following were recommended for the future research to focus on:

i. Considering variable viscosity

ii. Incorporate magnetized nanofluid flow through a channel with suction and injection at boundaries,

iii. Schmidt number effects on complex fluid flows can be investigated on turbulent or multiphase.

ACKNOWLEDGMENT

The authors profoundly appreciate individuals and all the lecturers of Usmanu Danfodiyo University, especially in the Department of Mathematics, Sokoto, Nigeria, for their dedication and contribution to shaping this research work.

REFERENCES

Abiodun, O. A. and Kabir, T. M. (2020).The combine effect of variable viscosity and variable thermal conductivity on natural convection couette flow. International Journal of thermo fluids, 5-6. **[Crossref]**

Agaie, B. G., Ndayawo, M. S., Usman, S., & Polytechnic, K. (2020). *Unsteady Magneto Poiseuille Oscillatory Flow Between Two Infinite Parallel Porous Plates.15*(2),56–61.

Amos, S. I., Mojeed T. A., Abubakar, Jos U. and Bidemi. O. F. (2020) MHD free convective heat and mass transfer flow of dissipative casson fluid with variable viscosity and thermal conductivity . Journal of Taibah University For Science, 14(1), 851-862. **[Crossref]**

Anuraddha, S. and Priyadhashini, P. (2016). MHD Free Convection Boundary Layer Flow of a Nanofluid Over a Permeable Shrinking Sheet in the Presence of Thermal Radiation &Chemical Reaction. Chemical and Process Engineering Research,46,18-26

Babu, P. R., Rao, J. A. and Sheri, S. (2014). The effect of radiation on MHD heat and mass transfer flow over a shrinking sheet with suction. Jounal of applied fluid mechanics, 7(4),641- 650. **[Crossref]**

Falade, J. A., Ukaegbu, J. C., Egere, A. C., & Adesanya, S. O. (2017). MHD oscillatory flow through a porous channel saturated with porous medium. *Alexandria Engineering Journal*, *56*(1), 147–152. **[Crossref]**

Gireesha, B. J. and Rudraswamy, N. G., (2014). The effect of Chemical reaction on MHD flow and heat transfer of a nanofluid near the stagnation point over a permeable stretching surface with non-uniform heat source/ sink. International Journal of Engineering, Science and Technology, 6(5),13-25. **[Crossref]**

Kareem, R. A and Salawu, S. O. (2017). The effects on Variable viscosity and Thermal conductivity effect of soret and dufour on inclined magnetic field in Non-Darcy Permeable Medium with dissipation. Journal of Mathematics and Computer Science, 22(3), 1-12. **[Crossref]**

Karwa, R. (2020). Heat and mass transfer. *Heat and Mass Transfer*, *59*(10), 1–1147. **[Crossref]**

Khaled, A. A., & Vafai. (2004). The effect of the slip condition on Stokes and Couette flows due to an oscillating wall: Exact solutions. *International Journal of Non-Linear Mechanics*, *39*(5), 795–809. **[Crossref]**

Makinde, O., D., Eegunjobi, A., S., and Tshehla, M., S. (2015). Thermodynamics Analysis of Variable Viscosity Hydro magnetic Couette Flow in a Rotating System with Hall Effects. Entropy, 17: 7811-7826. **[Crossref]**

Makinde, O., D., Tshehla, M., S., Iskander, T., Khan, W., A., and Mabood, F. (2016). MHD Couette-Poiseuille flow of variable viscosity Nano-fluids in a rotating permeable channel with Hall effects. Journal of Molecular Liquids, 221: 778–787. **[Crossref]**

Narsu, Silva kumar. And Rushikumar, B., (2020). The effect of MHD Chemically reacting unsteady flow over a radiated sheet with partial slip and variable thermal conductivity.AIP Conference Proceedings.1-10.

Noor, N. A. M., Admon, M. A., & Shafie, S. (2022). Unsteady MHD Squeezing Flow of Casson Fluid Over Horizontal Channel in Presence of Chemical Reaction. *Journal of Advanced Research in Fluid Mechanics and Thermal Sciences*, *92*(2), 49–60. **[Crossref]**

Noor, N. A. M., Shafie, S., & Admon, M. A. (2021). Impacts of chemical reaction on squeeze flow of MHD Jeffrey fluid in horizontal porous channel with slip condition. *Physica Scripta*, *96*(3). **[Crossref]**

Prakash, O. M., Makinde, O. D., Kumar, D., & Dwivedi, Y. K. (2015). Heat transfer to MHD oscillatory dusty fluid flow in a channel filled with a porous medium. *Sadhana - Academy Proceedings in Engineering Sciences*, *40*(4), 1273–1282. **[Crossref]**

Prakash, O., & Makinde, O. D. (2015a). MHD oscillatory Couette flow of dusty fluid in a channel filled with a porous medium with radiative heat and buoyancy force. *Latin American Applied Research*, *45*(3), 185–191. **[Crossref]**

Prakash, O., & Makinde, O. D. (2015b). Stokes' second problem. *Latin American Applied Research*, *45*(3), 185–191. **[Crossref]**

Quader, A. and Alam, M. (2021). Effect of unsteady MHD free Convective heat and mass transfer flow through a semi-infinite vertical porous plate in a rotating system with combined soret and dufour effects in the Presence of Hall current and constant heat flux. Journal of Applied Mathematics and Physics, 9, 1611-1638. **[Crossref]**

Rajashekar, M.N and Shankar Goud, B (2016). The effects of Chemical reaction on an unsteady MHD heat and mass transfer flow past a semi- infinite vertical porous moving plate in the presence of viscous dissipation. International Journal of Engineering Trends and Technology (IJETT), 42(8), 1-15. **[Crossref]**

Romanelli, G., Mignone, A., & Cervone, A. (2017). Pulsed fusion space propulsion: Computational Magneto-Hydro Dynamics of a multi-coil parabolic reaction chamber. *ActaAstronautica*, *139*(October)528-544. **[Crossref]**

Salawu, S. O., Abolarinwa, A., & Fenuga, O. J. (2020).

Transient analysis of radiative hydromagnetic poiseuille fluid flow of two-step exothermic chemical reaction through a porous channel with convective cooling. *Journal of Computational and Applied Research in Mechanical Engineering*,*10*(1), 51-62. **[Crossref]**

Seddek, M. A., and Salema, F. A. (2007). The effects of temperature dependent viscosity and thermal conductivity on unsteady MHD convective heat transfer past a semi- infinite vertical porous plate with variable suction. Computational Material Science,40(2),186- 192. **[Crossref]**

Sharma, B. K., Sharma, P. K., & Chauhan, S. K. (2022a). Effect of MHD on Unsteady Oscillatory Couette Flow Through Porous Media. *International Journal of Applied Mechanics and Engineering*, *27*(1), 188–202. **[Crossref]**

Sharma, T., Sharma, P., Seikh, A. H., Iqbal, A., & Kumar, N. (2023). Thermodynamical study of chemically-reactive and thermal-radiative magnetized oscillatory Couette flow in a porous medium filled channel. *Case Studies in Thermal Engineering*, *48*. **[Crossref]**

Uddin, M., & Murad, A. (2022). Stokes ' second problem and oscillatory Couette flow for a two-layer fluid : Analytical solutions. *Alexandria Engineering Journal*, *61*(12), 10197–10218. **[Crossref]**

Umavathi, J. C., & Anwar Bég, O. (2020). Effects of thermophysical properties on heat transfer at the interface of two immisicible fluids in a vertical duct: Numerical study. *International Journal of Heat and Mass Transfer*, *154*(June), 1–9. **[Crossref]**

UwantaI . J and Hamza M .M., (2014). Effect of suction / injection on unsteady hydromantic convective flow of reactive viscous fluid between vertical porous plates with thermal diffusion .Hindawi International Scholarly Research Notices,1—14. **[Crossref]**

Uwanta I. J. and Usman H. (2014).Effect of Variable thermal conductivity on heat and mass transfer flow over a vertical channel with magnetic field intensity.Journal of Applied and Computational Mathematics. 3(2),48-56.

Zubi, M. Al. (2018). MHD Heat and Mass Transfer of an Oscillatory Flow over a Vertical Permeable Plate in a Porous Medium with Chemical Reaction. *Modern Mechanical Engineering*, *08*(03), 179–191. **[Crossref]**

Zulkarnain, M., Sharudin, R. W. (2022). Towards understanding of pore properties of polystyrene-b-polybutadiene-b-polystyrene (SEBS) foam effect on thermal conductivity using numerical analysis. *International Journal of Technology,13*(3), 533–543. **[Crossref]**

APPENDIX

List of Constants

$$\alpha_1 = K_R Sc, \qquad \alpha_2 = K_R Sc - iwSc, \qquad \alpha_3 = P_r\, iw + R,$$

$$\alpha_4 = \sqrt{R} + \sqrt{\alpha_3}, \qquad \alpha_5 = \sqrt{R} - \sqrt{\alpha_3}, \qquad \alpha_6 = \sqrt{\alpha_3} - \sqrt{R}$$

$$A_1 = 1, \qquad A_2 = \frac{1-\cos(\alpha_1)}{\sin(\alpha_1)}, \qquad A_3 = 1, \qquad A_4 = -\cot(\alpha_2)$$

$$B_1 = 1 - B_2, \qquad B_2 = \frac{1-e^{\sqrt{R}}}{e^{\sqrt{R}} - e^{-\sqrt{R}}}, \qquad B_3 = -B_4 - B_5 - B_6, \qquad B_4 = \frac{2B_5 e^{2\sqrt{R}} + 2B_6 e^{-2\sqrt{R}}}{e^{-2\sqrt{R}} - e^{2\sqrt{R}}},$$

$$B_5 = \frac{-2B_1^2}{3} \qquad B_6 = \frac{-2B_2^2}{3} \qquad B_3^* = B_3 + B_5, \qquad B_4^* = B_4 + B_6$$

$$B_7 = 1 - B_8, \qquad B_8 = \frac{-e^{\sqrt{\alpha_3}}}{e^{-\sqrt{\alpha_3}} - e^{\sqrt{\alpha_3}}}, \qquad B_9 = -B_{10} - B_{11} - B_{12} - B_{13} - B_{14}$$

$$B_{10} = \frac{\left(B_{11} + B_{12} + B_{13} + B_{14}\right)e^{\sqrt{\alpha_3}} - B_{11}e^{\alpha_4} - B_{12}e^{-\alpha_4} - B_{13}e^{\alpha_5} - B_{14}e^{\alpha_6}}{\left(e^{-\sqrt{\alpha_3}} - e^{\sqrt{\alpha_3}}\right)}, B_{11} = \frac{K_9}{\alpha_4^2 - \alpha_3}, \qquad B_{12} = \frac{K_{10}}{\alpha_5^2 - \alpha_3}$$

$$B_{13} = \frac{K_{11}}{\alpha_5^2 - \alpha_3}, \qquad B_{14} = \frac{K_{12}}{\alpha_6^2 - \alpha_3},$$

$$K_1 = B_1 B_7 \alpha_3, \qquad K_2 = B_2 B_8 \alpha_3, \qquad K_3 = B_1 B_8 \alpha_3, \qquad K_4 = B_2 B_7 \alpha_3,$$

$$K_5 = B_1 B_7 \sqrt{R\alpha_3}, \qquad K_6 = B_1 B_8 \sqrt{R\alpha_3}, \qquad K_7 = B_2 B_8 \sqrt{R\alpha_3}, \qquad K_8 = B_2 B_7 \sqrt{R\alpha_3},$$

$$K_9 = -K_1 - 2K_5, \qquad K_{10} = -K_2 - 2K_6, \qquad K_{11} = -K_3 + 2K_7, \qquad K_{12} = -K_4 + 2K_8,$$

$$\mathrm{H}_1 = K + M, \qquad \mathrm{H}_2 = K + M + iw$$

$$D_1 = 1 - D_2 - D_3 - D_4 - D_5 - D_6^* - D_7^*, \qquad D_2 = \frac{U_q + L_2}{L_1},$$

$$D_3 = \frac{-G_r B_1}{R - H_1}, \qquad D_4 = \frac{-G_r B_2}{R - H_1}, \qquad D_5 = \frac{-G_c A_1}{\alpha_1 + H_1}, \qquad D_6 = \frac{-G_c A_2}{\alpha_1 + H_1}$$

$$D_6^* = \frac{-G_r Vm B_3^*}{4R - H_1}, \qquad D_7^* = \frac{-G_r Vm B_4^*}{4R - H_1}, \qquad D_7 = 1 - D_8 - L_{11}, \qquad D_8 = \frac{L_{11} e^{\sqrt{H_2}} - e^{\sqrt{H_2}} - L_{12}}{e^{-\sqrt{H_2}} - e^{\sqrt{H_2}}}$$

$$D_9 = \frac{-L_3}{\alpha_3 - H_2}, \qquad D_{10} = \frac{-L_4}{\alpha_3 - H_2}, \qquad D_{11} = \frac{-L_5}{\alpha_4^2 - H_2}, \qquad D_{12} = \frac{-L_6}{\alpha_4^2 - H_2},$$

$$D_{13} = \frac{-L_7}{\alpha_5^2 - H_2}, \qquad D_{14} = \frac{-L_8}{\alpha_6^2 - H_2}, \qquad D_{15} = \frac{L_9}{\alpha_2 + H_2}, \qquad D_{16} = \frac{L_{10}}{\alpha_2 + H_2}$$

$$L_1 = e^{-\sqrt{H_1}} - e^{\sqrt{H_1}},$$

$$L_2 = \left(D_3 + D_4 + D_5\right) e^{\sqrt{H_1}} - e^{\sqrt{H_1}} - D_3 e^{\sqrt{R}} - D_4 e^{-\sqrt{R}} - D_5 \cos(\alpha_1) - D_6 \sin(\alpha_1) - D_6^* e^{2\sqrt{R}} - D_7^* e^{-2\sqrt{R}}$$

$$L_3 = G_r B_7 + G_r B_9 Vm, \qquad L_4 = G_r B_8 + G_r B_{10} Vm, \qquad L_5 = G_r B_{11} Vm, \qquad L_6 = G_r B_{12} Vm,$$

$$L_7 = G_r B_{13} Vm, \qquad L_8 = G_r B_{14} Vm, \qquad L_9 = G_c A_3, \qquad L_{10} = G_c A_4,$$

$$L_{11} = D_9 + D_{10} + D_{11} + D_{12} + D_{13} + D_{14} + D_{15}$$

$$L_{12} = D_9 e^{\sqrt{\alpha_3}} + D_{10} e^{-\sqrt{\alpha_3}} + D_{11} e^{\alpha_4} + D_{12} e^{-\alpha_4} + D_{13} e^{\alpha_5} + D_{14} e^{\alpha_6} + D_{15} \cos(\sqrt{\alpha_2}) + D_{16} \sin(\sqrt{\alpha_2})$$